SAE Aero Design East 2024
Design Report

March 4, 2024

The University of British Columbia

UBC AeroDesign

Team 313- Micro Class

Team Captain:

Thenushaa Balasingam & Bryson Wu

Design Team Members:

Eric Zhang, Alanna Lu, Eric Kondor, Josh Marwaha, Gabriel Lee, Michelle Nguyen, Kevin Wang, Thenushaa Balasingam, Yuri Bendall, Yoonha Lee, Neha Bal, Lindy Shi, Evan Comba, Nic Chu, Hannah Saarimaki, Julia Shaw, Vansh Sharma, Justin Yoon, Ella Yan

Statement of Compliance

APPENDIX A - STATEMENT OF COMPLIANCE

Certification of Qualification

Team Name	**UBC AeroDesign Micro**	Team Number	**313**
School	**The University of British Columbia**		
Faculty Advisor	**Carl Ollivier-Gooch**		
Faculty Advisor's Email	**cfog@mech.ubc.ca**		

Statement of Compliance

As faculty Adviser:

CFO-G (Initial) I certify that the registered team members are enrolled in collegiate courses.

CFO-G (Initial) I certify that this team has designed and constructed the radio-controlled aircraft in the past nine (9) months with the intention to use this aircraft in the **2024** SAE Aero Design competition, without direct assistance from professional engineers, R/C model experts, and/or related professionals.

CFO-G (Initial) I certify that this year's Design Report has original content written by members of this year's team.

CFO-G (Initial) I certify that all reused content have been properly referenced and is in compliance with the University's plagiarism and reuse policies.

CFO-G (Initial) I certify that the team has used the Aero Design inspection checklist to inspect their aircraft before arrival at Technical Inspection and that the team will present this completed checklist, signed by the Faculty Advisor or Team Captain, to the inspectors before Technical Inspection begins.

Carl Ollivier-Gooch — 2024-02-29

Signature of Faculty Advisor — Date

2024-02-24

Signature of Team Captain — Date

Table of Contents

List of Figures

List of Tables

1. Executive Summary

This report documents the UBCAD Micro Class aircraft, *Sonic*, for the 2023-2024 SAE Aero Design West Micro Class Competition. This year our team decided to switch to a new class to increase the rate and quality of prototypes which would allow us to produce a more competitive design. The team's objective this year is to gain experience designing, manufacturing, and testing structures through validating design analysis with iterative prototypes. *Sonic* features an inverted U-tail configuration with a 33” wingspan. *Sonic* is designed to have an empty weight of 2.6lb, a maximum take-off weight of 7.6lb and can carry a total of 5lb of water. With 5 payload configurations, *Sonic* is robust, reliable, and can achieve a maximum estimated score of 26.1 per flight round, enabling our team to earn a top-five placement in the competition. The following sections describe the design, manufacturing, and testing that UBCAD conducted to prepare *Sonic* for competition.

Figure 1.1: Render of *Sonic*

2. List of symbols and acronyms

α, AoA	Angle of Attack
AR	Aspect Ratio
C	Chord
C_D	Combined Aircraft Drag Coefficient
$C_{D,max}$	Maximum Combined Aircraft Drag Coefficient
$C_{D,min}$	Component Drag
C_{HT}	Tail Volume Coefficient for Horizontal Tail
C_l	Lift Coefficient for 2D Section Profile
C_L	Lift Coefficient for Finite Aspect Ratio Wing
$C_{L\alpha}$	Slope of Lift vs. Angle of Attack Curve for Finite Aspect Ratio Wing
$C_{L,max}$	Lift Coefficient at Maximum Angle of Attack for Finite Aspect Ratio Wing
C_M	Moment Coefficient
CF	Carbon Fibre
C_{VT}	Tail Volume Coefficient for Vertical Tail
CG	Centre of Gravity
FMEA	Failure Mode and Effects Analysis
FoS	Factor of Safety
HT	Horizontal Tail
LLT	Lifting Line Theory
MAAC	Model Aeronautics Association of Canada
MAC	Mean Aerodynamic Chord
MCRC	Micro Class
MLG	Main Landing Gear
MTOW	Maximum Take-off Weight
NP	Neutral Point
PWT	Parkinson Wind Tunnel
PLA	Polylactic Acid
Re	Reynolds Number
SM	Static Margin
TLG	Tail Landing Gear
TO	Take-off
TPU	Thermoplastic Polyurethane
UBCAD	UBC AeroDesign
VT	Vertical Tail
VTOL	Vertical takeoff and landing
W	Weight
WBS	Work Breakdown Structure
WDM	Weighted Decision Matrix
x_{CG}	Longitudinal Centre of Gravity Location
x_{NP}	Longitudinal Location of Neutral Point
λ	Taper Ratio

3. Referenced Documents & Specifications

[1] Gudmundsson, S. (2014). General Aviation Aircraft Design: Applied Methods and Procedures. Elsevier.

[2] Selig, M. (n.d.). UIUC Airfoil Coordinates Database. University of Illinois at Urbana-Champaign. Retrieved July 16,
2023, from https://m-selig.ae.illinois.edu/ads/coord_database.html

[3] Sadraey, M. H. (2013). Aircraft Design - A Systems Engineering Approach. West Sussex: John Wiley & Sons Ltd.

[4] Nicolai, L. M. (2009). Estimating R/C Model Aerodynamics and Performance", Lockheed Martin Aeronautical Company.

[5] Glauert, H. (1948). The Elements of Aerofoil and Airscrew Theory, 2nd ed. Cambridge: Cambridge University Press.

[6] Nugroho, G., Zuliardiansyah, G., & Rasyiddin, A. A. (2022). Performance analysis of empennage configurations on a surveillance and monitoring mission of a VTOL-plane UAV using a computational fluid dynamics simulation. MDPI. Retrieved from https://www.mdpi.com/2226-4310/9/4/208

[7] Raymer, D.P. (2018). Aircraft Design: A Conceptual Approach (6th ed.). American Institute of Aeronautics and Astronautics.

[8] Gueraiche, D., & Popov, S. (2017). Winglet Geometry Impact on DLR-F4 Aerodynamics and an Analysis of a Hyperbolic Winglet Concept. *Aerospace*, *4*(4), 60. MDPI AG. Retrieved from http://dx.doi.org/10.3390/aerospace4040060

[9] Staples, G. (2013). Propeller Static & Dynamic Thrust Calculation. *ElectricRCAircraftGuy*. https://www.electricrcaircraftguy.com/2013/09/propeller-static-dynamic-thrust-equation.html

[10] Beer, F. P., Johnston, E. R., DeWolf, J. T., & Mazurek, D. F. (2020). Mechanics of Materials. McGraw-Hill Education.

[11] MIL-F-8785C. (1980). Military Specification: Flying Qualities of Piloted Airplanes.

[12] Ashby, M.F. (1999). Materials Selection in Mechanical Design, 2nd ed., Oxford: Butterworth-Heinemann

4. Project Management

4.1 Team Organization & Work Breakdown Structure

Our team developed a Work Breakdown Structure (WBS), which alongside a detailed dynamic timeline, ensures the timely completion of all deliverables. The WBS involves breaking down tasks into manageable packages, facilitating progress tracking, and offering a comprehensive overview of all subteam activities seen in Figure 4.1.1.

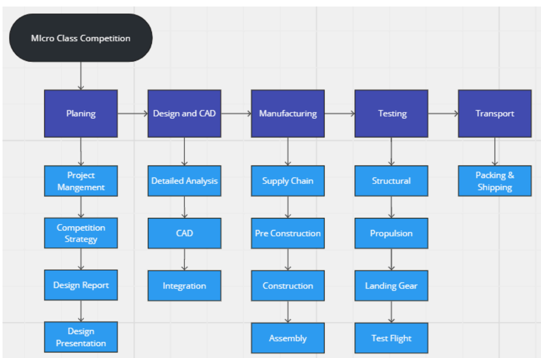

1	**Design and CAD**	2	**Manufacturing**	3	**Testing**
1.1	**Airfoils**	2.1	**Supply Chain**	3.1	**Structural**
	Management	2.1.001	Purchase Wood and Glue	3.1.001	Wing Bending and Torsion
1.1.001	SOLIDWORKS Training and CWSA	2.1.002	Purchase Spar	3.1.002	Wingtip Loading
1.1.002	AutoCAD/Lasercut Training	2.1.003	Purchase Metal	3.1.003	Fuselage Bending and Torsion
1.1.003	XFLR5 Training	2.1.004	Purchase hardware	3.1.004	Fuselage Payload Test
1.1.004	Airfoils EBOM	2.1.005	Purchase electronics		
1.1.007	Instructional Videos	2.1.006	Purchase safety and equipment	3.2	**Propulsion**
				3.2.001	Propulsion Test Rig
	Analysis	2.2	**Pre-Construction**	3.2.002	Static Thrust
1.1.101	Airfoil Selection / Design		**Build Plan**	3.2.003	Dynamic Thrust (Wind Tunnel)
1.1.102	3D Finite AR Correction	2.2.001	Wing Build Plan	3.2.004	Pixha
1.1.103	3D Wing Sizing & Analysis	2.2.002	Vertical Stab Build Plan		
1.1.104	3D Lift Methods Comparison	2.2.003	Horizontal Stab Build Plan	3.3	**Landing Gear**
1.1.105	Control Surface Sizing	2.2.004	Front Compartment Build Plan	3.3.001	Drop Test with weights
1.1.106	Tail Airfoil Selection / Design	2.2.005	Main Compartment Build Plan	3.3.002	Fully Loaded Drop Test
1.1.107	Tail Sizing	2.2.006	Tail Compartment Build Plan	3.3.003	Steering
1.1.108	Spar Sizing	2.2.007	Hatch Build Plan	3.3.004	Landing Gear Static Deflection
1.1.109	Rib spacing / other structural analysis	2.2.008	Landing Gear Building Plan		
1.1.110	Servo Sizing	2.2.009	Payload Build Plan	3.4	**Miscellaneous**
1.1.111	Dynamic Stability	2.2.010	Wire Routing	3.5.001	Loading/Unloading
1.1.112	Drag Polar	2.2.011	Electrical Schematics	3.5.002	Shipping container fit
1.1.113	Wingtips		**DXF Files**		
1.1.114	Structural Enhancement Study	2.2.101	Wing	3.5	**Test Flight**
1.1.115	Flaps	2.2.102	Vertical Stab	3.6.001	Pre-Flight Checklist

Figure 4.1.1 **(left)** WBS Categories & Figure 4.1.2 **(right)** Sample Detailed WBS Sections

4.2 Schedule & Budget

With this year's competition class change from regular class within our design team in combination with the 3-year rule change this year, our team focused on short preliminary projects during the summer months. These projects consisted of FMEA of past MCRC plane crashes at competition, CF manufacturing training, and analysis of varying types of wingtips for a smaller plane. Around the preliminary design phase, an initial timeline was created and modified as the design matured as seen below in Figure 4.2.1. The initial timeline was planned around two test flights; one before the design report and the other before the competition. This provides the opportunity to iterate on our initial design and also complete a full cycle flight with the competition plane in preparation.

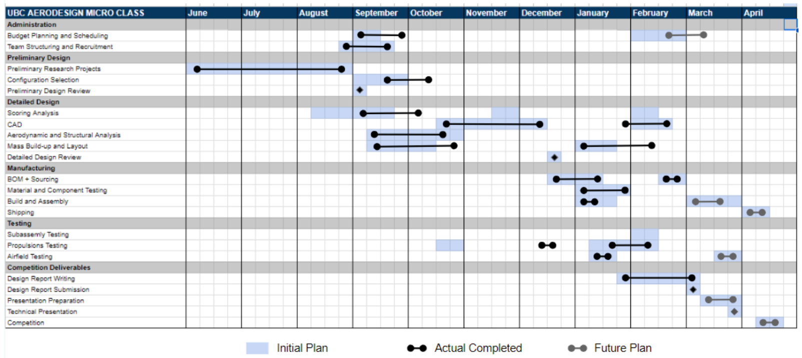

Figure 4.2.1: High-level Gantt Chart, Showing Planned, Completed, and Future Timelines.

UBCAD receives approximately 50% of its funding yearly from the University and the remainder from external organizations. The total budget is then allocated amongst the other class teams, where the MCRC team operates within a budget of CA$ 2,000 divided proportionally among the subteams and allocated for general construction.

5. Design Layout & Trade Studies

5.1 Derivation of Requirements

The mission requirement for the MCRC plane is to take off within the 100ft runaway limit, turn and cruise, and land safely within 200ft. After landing, water must be released from the payload container within 1 minute. UBCAD follows a 3-year rule set design objectives encompassing the following, *Year 1:* Reliability, (minimize risk), *Year 2:* Completeness of system, and *Year 3:* Optimization. All the aircraft design objectives are summarized below.

Table 5.1: Summary of aircraft design objectives.

Scoring Requirements	SAE Requirements	Flight Plan Constraints
Minimize wingspan & Empty Weight Minimize Takeoff Distance Maximize Liquid Payload	Maximum 450W Power Draw 67 fluid ounces payload container	Must take-off within 100ft Must land within 200ft

To fulfill the design objectives, UBCAD developed a mission profile diagram to extract precise competition and aerodynamic requirements shown in Figure 5.1.1 and a flight envelope to address structural requirements in section 7. UBCAD also established a Maximum Takeoff Weight (MTOW) of 7.6lb, which provides the opportunity to work up to a competitive and high-scoring design. The MTOW was finalized after the primary prototype, which allowed us to determine a feasible empty weight to manufacture. Additionally, scoring analysis was based on a 10ft runway takeoff, to maximize potential points in all possible payload configurations.

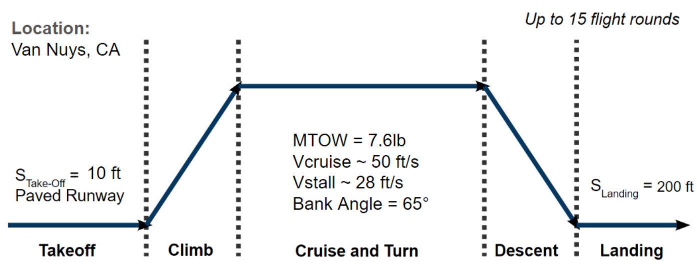

Figure 5.1.1: Sonic's Mission Profile Diagram

An aspect ratio of 4 was selected to help minimize the wingspan with high lift, verified with preliminary XFLR5 finite wing analysis. A load factor of 3 was also decided based on Raymer's[] chart of common load factor for transport aircraft.

5.2 Scoring Analysis

Design parameters were then determined and optimized using Gudmundsson's constraint diagram literature [1]. MTOW and required thrust were calculated at varying wingspans, using preliminary lift values derived from XFLR5, resulting in a wingspan of 33in. The constraint diagram (Figure 5.2.1) marks a red star at the ideally designed flight case, where all flight conditions are met, while vertically constrained by the wing span. The wing loading is capped at 4.01lb/ft^2 and thrust to weight at 0.39. Which requires about ~ 3 lbs of thrust. After a discussion with our test flight pilot after a hop test, the required thrust was increased to 4 lbs with a safety factor of 1.3, to ensure a short takeoff with a fully loaded plane.

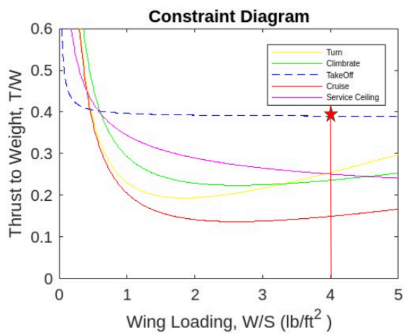

	0 ≤ x ≤ 10 ft	10 ≤ x ≤ 25 ft	25 ≤ x ≤ 50 ft	50 ≤ x ≤ 100
Btakeoff	20	15	9	0
Flight Score	26.12	21.12	15.12	6.12
M	0.7118082518			
Wpayload (lbs)	5			
Z	15.44	10.44	4.44	-4.56
Wempty (lbs)	2.6			
Span (ft)	2.75			
MTOW	7.6			

Figure 5.2.1: (left) Sonic's Mission Profile Diagram & **(right)** Scores at varying takeoff distances

With the following constraints and parameters, *Sonic* would score 26.12 pts if the plane takes off within 10 ft as designed. All other conditions can be seen in Figure 5.2.1.

5.3 Configuration Selection and Trade Studies

To select the configuration of *Sonic*, UBCAD conceptualized subassembly fragments and interwove them into four preliminary concepts as shown in Table 5.4.1. Each concept consists of a blended wing body configuration due to its increased aerodynamic efficiency and greatest payload capacity.

Table 5.4.1: Summary of Configurations Considered for Trade Studies.

Parameters	Blended Wing U-Tail	Blended Wing Inverse U-Tail	Blended Wing Conventional Tail Twin Boom	Blended Wing U-Tail Twin Boom
Wing Height	High	High	High	High
Tail Boom	Single	Single	Twin	Twin
Fuselage Shape	Blended Wing Body	Blended Wing Body	Blended Wing Body	Blended Wing Body
Tail Configuration	U-Tail	Inverse U-Tail	Conventional	U-Tail
LG Configuration	Tricycle	Tricycle	Tricycle	Tricycle

UBCAD implemented the scoring analysis described in Section 5.3.2 to assign the weightings of five evaluation criteria in a Weighted Decision Matrix (WDM), as described in Table 5.4.2, and score the initial concepts. Empty weight was a priority in the configuration selection process followed by stability and payload capacity/integration. Due to this criteria, configurations such as the 'Blended Wing U-Tail' were eliminated due to difficulty in payload integration and decreased stability.

Table 5.4.2: WDM Weightings for Trade Studies.

Empty Weight	Wing Span	Aerodynamic Efficiency	Payload Removal and Capacity	Manufacturability	Stability and Control
21.5%	11.6%	12.6%	15.7%	21.9%	16.7%

Of the four initial concepts, the blended wing body with an inverse U-tail scored the highest as it minimizes empty weight and maximizes take off and aerodynamic efficiency, stability, and payload capacity.

6. Design Sizing and Optimization

6.1 Airfoil Selection

UBCAD considered twenty-six airfoils from the University of Illinois at Urbana-Champaign airfoil database [2]. Desired aerodynamic properties across all airfoils included a high C_L/C_D ratio, good stall performance, and a low moment coefficient, analyzed at low Re (Reynolds numbers).

For the wing, the maximum section C_L and C_L/C_D ratio for the root airfoil were prioritized because of their high capacity to increase the aircraft's MTOW. At the wingtip, an airfoil with excellent stall characteristics was chosen so the root would stall first. Using XFLR5's XFOIL direct analysis feature to analyze airfoils at a Re of 200k with our ranking criteria, a root airfoil S1223 and the E591 at the tip was identified, These airfoils were combined in various 3D combinations to evaluate their synergistic performance, accounting for the effect of the aerodynamic twist. For the tail, an airfoil with a large C_l vs. Angle of Attack (AoA) slope for responsiveness and a high stall angle is desirable. Following a similar process to the wing airfoil selection, NACA0018 was selected for the HT and VT. Figure 6.1.1 describes key aerodynamic properties of our airfoils.

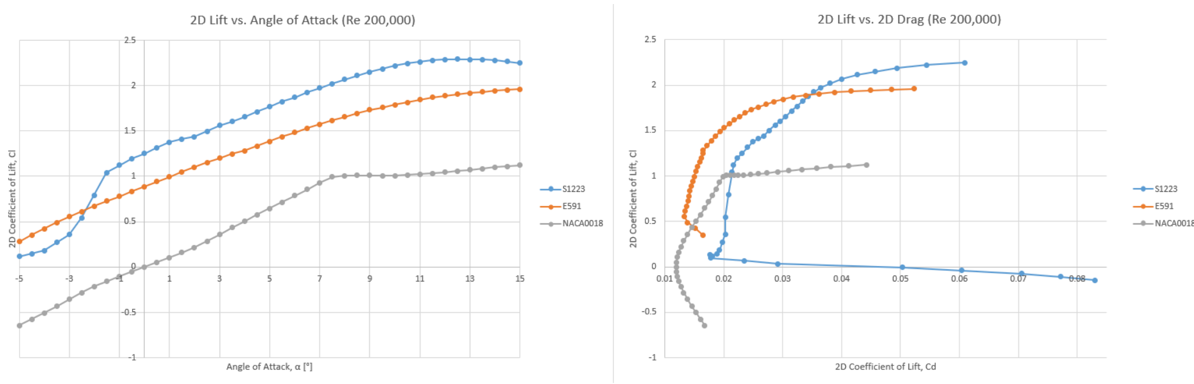

Figure 6.1.1 (left) XFLR5 2D Lift vs. AoA for Airfoils at Re = 200K & **(right)** XFLR5 2D Lift vs. Drag for Airfoils at Re = 200K

6.2 Wing Sizing

The UBCAD MCRC wing sizing aimed to select a wingspan and AR combination for further analysis based on their predicted scoring characteristics. In section 5.3.2, the scoring analysis defined a constraint on the wingspan at 33in and an AR of 4, which were both derived from multiple takeoff calculations, allowing the plane to fly with minimal thrust and within wingspan constraints.

6.3 Wing Sizing and Planform Design

To maximize 3D wing performance, UBCAD performed a rigorous XFLR5 analysis on the top two airfoil choices: the S1223 root with a S1223 RTL tip, and S1223 root with an E591 tip. Using the XFLR5 VLM1 Horseshoe Vortex analysis, a 3D finite wing was developed primarily optimizing $C_{L,max}$ and $C_{D,min}$ as well as the $C_{M,min}$, and Oswald efficiency.

Wing geometry was optimized numerically in three iterations. First, the tip-to-root taper and the aspect ratio (AR) of 4.00 were fixed to optimize the spanwise taper location from the root in terms of the above parameters. This location was fixed to optimize the tip to root taper. Finally, the optimized tip to root taper was used to repeat the first iteration and optimize synergistically. This last iteration converged to the same spanwise taper location as the first. UBCAD is thus confident in the accuracy of the analysis and concludes that the S1223 root with an E591 tip is the optimal configuration with a tip-to-root taper ratio of 75% (possessing a root chord of 8.57 inches and tip chord of 6.429 inches). The optimized monoplane planform features an aerodynamic twist with a $C_{L,max}$ of 1.00, a $C_{D,min}$ of 0.108, a $C_{M,min}$ of -0.586, and an Oswald efficiency of 1.02. Geometric twists, sweeps, and other geometric features were not incorporated into our design because they contribute minimally to subsonic flight [3] and significantly detriment manufacturability.

Subsequently, the XFLR5 output was validated against multiple other methods presented by [4,5], performed at AR of 4.0 (Figure 6.3.1).

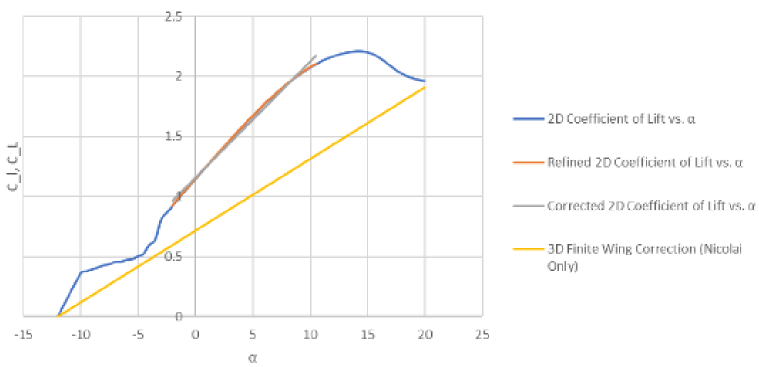

Figure 6.3.1: XFLR5 LLT vs. 3D Finite Wing Correction C_L Predictions.

6.4 Tail Sizing

An inverted U-tail configuration was selected for this aircraft due to its increased HT efficiency. With a tail arm of 12.87" and a tail efficiency coefficient of η = 0.5, the HT is lifted above the wake of the fuselage due to the inverted U-tail configuration. Since the tail arm of this aircraft is smaller than the distance between the main spar and trailing edge of the fuselage airfoil, direct integration into the fuselage's airfoil without the need for a tail boom or rod is possible. Applying the tail volume coefficients for an inverted U-tail configuration from Nugroho et al.'s paper on empennage configurations of a VTOL plane [6], the following tail values were produced: AR,HT = 3.0, AR, VT= 2.0 , C, HT = 0.6, C, VT = 0.04 . Using a method similar to wing sizing, dimensions for the VT and HT were determined by first setting the taper ratio and then the span-to-taper ratio. The HT was designed without taper, featuring a 5.09 inch chord. The two VTs were designed with a 0.7 taper ratio each, having a root chord of 4.39 inches and a tip chord of 3.08 inches.

6.5 Servo Sizing

To select the ideal servos, we first needed to calculate the required torque to deflect each control surface by ± 30°. This was done by calculating the pressures acting on the top and bottom of the control surface when at maximum deflection and a top speed of 40 ft/s. The pressures were found using XFLR5. Using the known moment arm of the servo, the required torque for each control surface was found. The ailerons require ~ 2 oz-in of torque at full deflection. The HT and VT require less torque ~ 1 oz-in. A minimum safety factor of 4 was applied to each control surface, as unexpected pressure variations could exceed the calculated tolerable torque. These values were also checked against an online servo calculator which yielded only slightly smaller values.

6.6 Subassembly Sizing and Interfaces

The payload container dimensions were the primary sizing constraints of the aircraft, thus we aimed to minimize internal volume, while still containing the payload and electrical systems. Additional space was allocated to place components in a manner that complied with our stability analyses. UBCAD also considered the logistical requirements of transporting the plane to and from the competition. The aircraft was built as a single unit without disassembly for transport, minimizing failure risks by avoiding detachable components like bolts. Stress analysis and tests were conducted to confirm the structural integrity of these permanent interfaces.

7. Analysis & System Testing

7.1 Drag Analysis

UBCAD performed a complete aerodynamic analysis, including the creation of a comprehensive drag polar (Fig. 7.1.1.) to validate drag estimates made using both the Raymer and Nicolai method from the preliminary design stage [7]. The $C_{D,min}$ was determined using the component drag build-up method [1] shown in table 7.1.1. To model a complete aircraft drag polar, the induced drag factor was calculated based on an aspect ratio of 4 and an Oswald efficiency factor of 1. The viscous factor was determined by plotting C_D and $(C_L\text{-}C_{L,min})^2$ with 2D S1223 data. The resulting full-drag polar confirms that Sonic possesses excellent drag characteristics.

Component	$C_{D,min}$
Fuselage	0.0109
Wing	0.0102
HStab.	0.0012
VStab.	0.0010
Landing Gear	0.0002
Total	**0.0241**

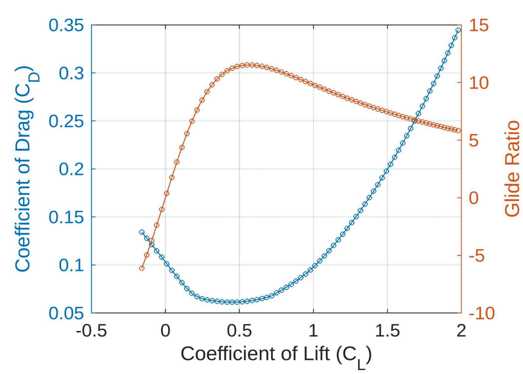

Table 7.1.1. : CD,min from Different Plane Compartment
Figure 7.1.1. : Total Drag Polar

7.2 Runway/takeoff performance

Take-off represents a critical design constraint due to short wingspan and takeoff length, so a thorough analysis and validation process was conducted. Using the drag data derived during wing sizing in XFLR5

(Section 6.3), and the motor curve obtained from dynamic testing from Section 8.6, the ground roll was calculated and compared using analytical methods [3] and validated with a forward Euler iterative scheme. Sonic can take off in ~10ft with full elevator deflections using the most conservative method and FoS of 1.2, to account for “non-straight” thrust angle effects.

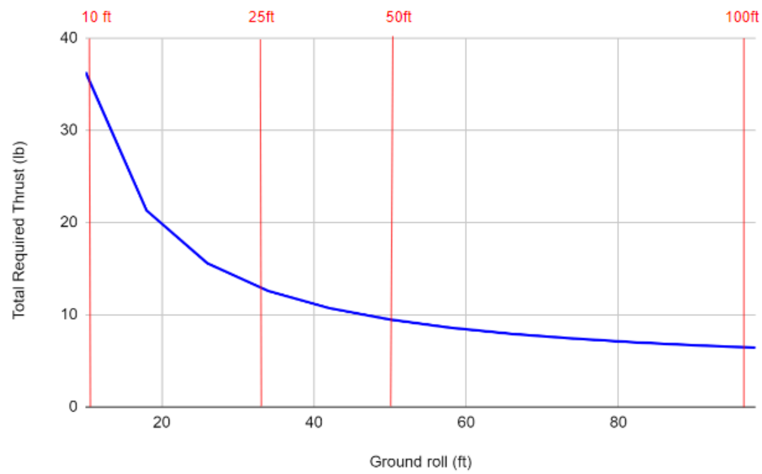

Figure 7.2.2: (left) Dynamic Thrust at Takeoff vs Ground Roll

7.3 Flight Maneuver Performance

Sadraey’s critical value method [3] was implemented in MATLAB to compute the control to lifting surface ratio. To optimize in-flight maneuverability, the aircraft must achieve the design requirements specified in Table 7.3.1, given maximum deflection angle and performance parameters derived using methods from Sadraey’s textbook. This yielded the sizing estimates seen in Figure 7.3.1.

Table 7.3.1: *Sonic* Control Surface Sizing.

Control Surface	Control-to-Lifting Surface Chord Ratio	Maximum Deflection Angle	Performance Parameter	Projected Performance
Ailerons	16.9%	20°	Banking time to 30°	~ 1.8s
Elevators	40%	20°	Moment produced about CG at full deflection	1.33 lb/ft
Rudder	50%	30°	Cross-wind speed for deflection angle < 30°	Cross-wind < 15.45 mph

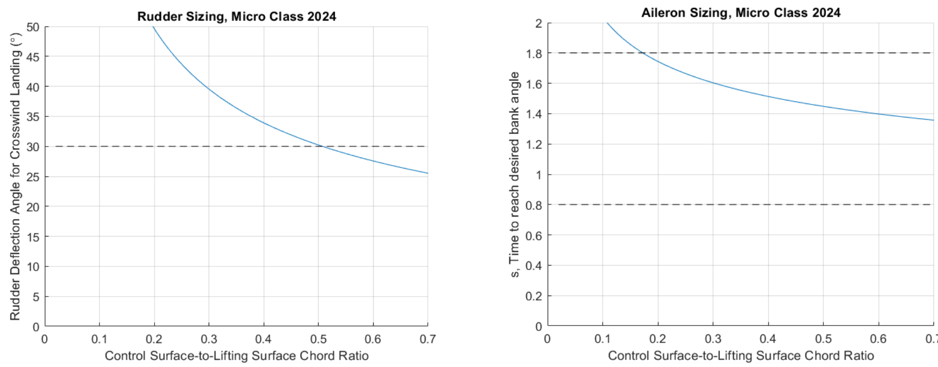

Figure 7.3.1: (left) Rudder Deflection Angle vs. Control Surface to Lifting Surface Chord Ratio & **(right)** Time to Reach Desired Bank Angle vs. Control Surface to Lifting Surface Chord Ratio.

7.4 Winglet Optimization

Winglets are known to reduce drag by minimizing wingtip vortices produced by the difference in air pressure above and below the wing. UBCAD used Ansys Fluent CFD to analyze 10 different configurations of blended, canted, and raked winglets, chosen based on previous CFD studies on winglets [8]. We normalized the length of each winglet and ranked them according to the performance index I_{WP}. Figure 7.4.1. shows the rank of each of these wingtips, with a 65% weight on C_L/C_D and a 35% weight on wingspan conservation.

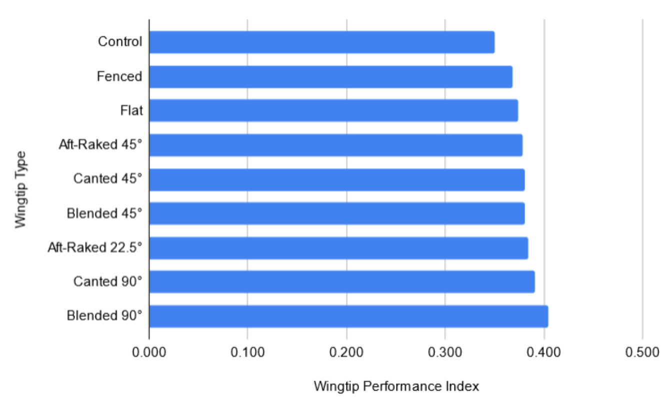

$$I_{WP} = Weight_{Aerodynamic\ Performance} \times \frac{(C_L/C_D)_{Configuration}}{(C_L/C_D)_{Control}} + Weight_{Length} \times \frac{Wing\ Span_{Configuration}}{Wing\ Span_{Control}}$$

Figure 7.4.1: (bottom) Performance index equation and **(top)** results for various winglet configurations

The preliminary results shown in Figure 7.4.2 led us to optimise a blended 90 degree winglet configuration.

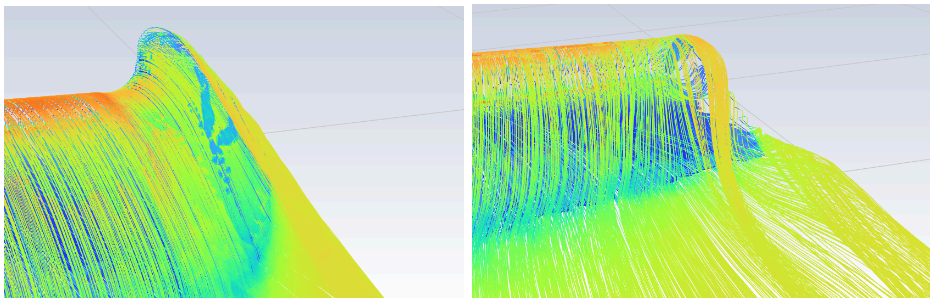

Figure 7.4.2: (left) Ansys Fluent CFD air velocity simulation showing small vortex with winglet and **(right)** large vortex w/o winglet

For our final plane, we determined a blended 90° winglet would increase the plane's C_L/C_D by 6.5%, while only taking up 6% of the total wingspan.

7.5 Propulsion Performance & Testing

T-Motor AT2321 with an APC 10"x7" propeller produces the most thrust with the given constraints: a minimum thrust of 3 lbs at 450 W as required in Section 5.2, rated power of 450 W - 750 W and a weight under 0.35 lbs. The range of the propeller sizes was determined using the equation below (Figure 7.5.1) and manufacturer's RPM limits. The equation assumes zero-thrust freestream velocity V_0 is equal to airflow speed leaving the propeller blade. The equation also uses an empirically tested correction factor [9].

$$F = 4.392399 * 10^{-8} * RPM\left(\frac{diameter^{3.5}}{\sqrt{pitch}}\right)\left(4.23333 * 10^{-4} * RPM * pitch - Vo\right)$$

Figure 7.5.1: Thrust Approximation Equation

Successful power plants were tested by attaching a motor to a thrust stand with a load cell and placing it in a wind tunnel. All tests were conducted at 100% throttle using a 2200mAh, 4s LiPo battery, with around or above 3.9V per cell. A 450-watt power limiter was used, and no fuselage blockage was present during testing. Figure 7.5.1. conveys the static thrust results for various power-plants.

AT2310		**AT2317**		**AT2321**	
Combination	Thrust (lbs)	Combination	Thrust (lbs)	Combination	Thrust (lbs)
AT2310 & 6x4	2.0	AT2317 & 9x4.5	3.8	AT2321 & 9x4.5	4.4
AT2310 & 6x6	2.0	AT2317 & 9x7.5	3.6	AT2321 & 9x7.5	4.2
AT2310 7x4	3.6	AT2317 & 9x9	3.1	AT2321 & 9x9	3.8
AT2310 & 7x5	3.4	AT2317 & 10x5	4.5	AT2321 & 10x5	5.2
AT2310 & 7x7	2.7	AT2317 & 10x7	4.4	AT2321 & 10x7	5.1

Table 7.5.1. : Static thrust test results.

Dynamic thrust data was then gathered for the top-performing power plants.

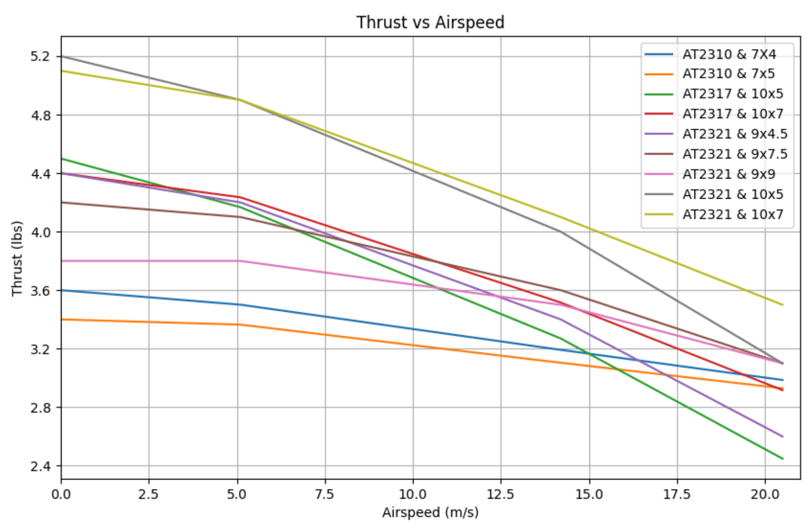

Figure 7.5.2 : Dynamic thrust results in a wind tunnel with the motor running at 100% throttle with varying airspeed.

The combination of a T-Motor AT2321 with an APC 10”x7” propeller was selected for its high thrust performance at high airspeeds (Figure 7.5.2). It lags in thrust at 0 airspeed compared to the APC 10”x5” propeller but outperforms the APC 10”x5” propeller at higher airspeeds.

7.6 Wing Spar Sizing & Testing

UBCAD used a carbon fibre hollow tube as the aircraft's wing spar to support the flight forces acting on the lifting surface. The carbon fibre hollow tube configuration was selected based on the high strength-to-weight ratio of composites and its manufacturability [10]. Through an XFLR5 horseshoe vortex analysis, the bending moments acting at each point of the wing were determined and used to calculate the stresses acting on the given points (Figure 7.6.1.). Then the stress values were used to size the diameter of the hollow tube spar according to a sufficient FoS of at least 1.5. The same processes were repeated for the spar sizing of the empennage components. For manufacturing simplicity, the tail's spar configuration opted for a composite I-beam with balsa webbings and basswood spar caps. The selection process of spar sizes also considered the availability of carbon fibre tube diameters and the dimensions necessary to support the rib's height [7].

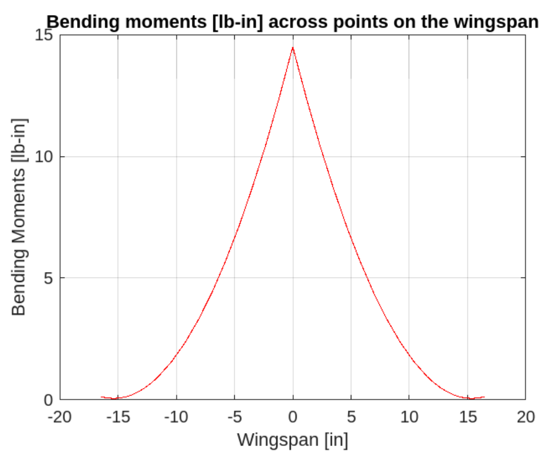

Figure 7.6.1. Bending moments with for points across the wingspan

UBCAD verified the spar sizing analysis by conducting a three-point load test which evaluated the maximum deflections and the strength of the spar. The spar was supported on both ends and weights were applied to the center of the spar (Figure 7.6.2. Right). The maximum deflection, which occurred at the center of the spar, was then measured. The results of the three-point load test showed that the actual measured deflections were less than the theoretical deflections (Figure 7.6.2. Left), and the spar did not sustain any plastic deformation.

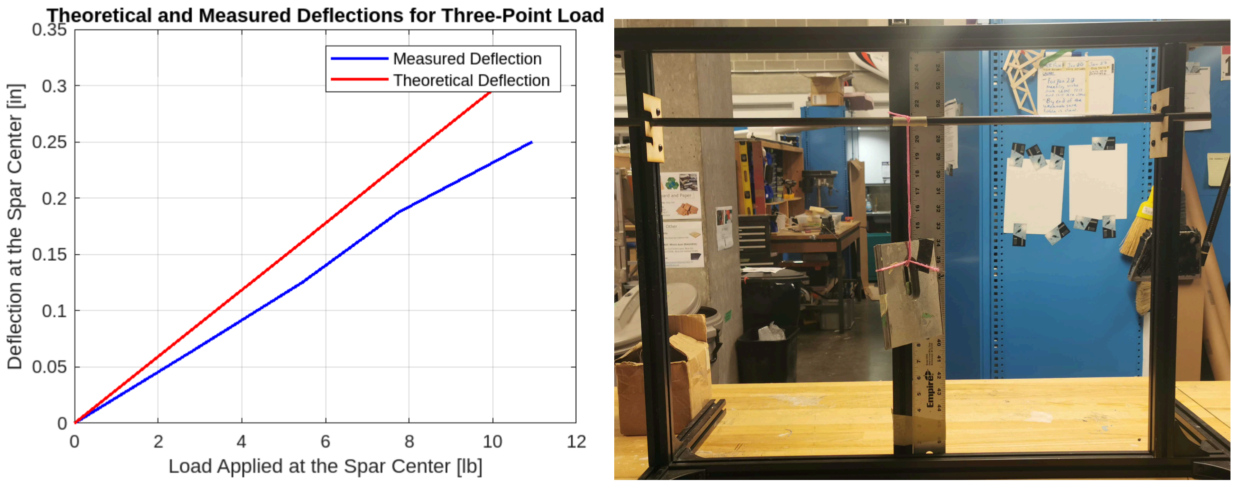

Figure 7.6.2: (left) Theoretical and **(right)** Measured Deflections for Three-Point Load Test and Three-Point Load Test Setup

7.7 Fuselage Sizing & Testing

As weight is a significant constraint, the fuselage was sized to be as sleek as possible. Key to this design were two plywood ribs spanning the payload container's width, serving as the primary longitudinal structural members. UBCAD optimized the thickness and width of these ribs using SolidWorks simulations and testing. A fuselage length of 25" was selected after several iterations of layout to find a balance between aerodynamic stability and structural strength. Stiffeners were used to increase the stiffness along the lateral axis, and mitigate twisting. The team conducted shear and bending analysis to determine the optimal number and size of key stiffeners. Stiffeners directly supporting the weight of the payload, main ribs, and the motor mount were chosen to be plywood, while balsa was used elsewhere to meet weight constraints.

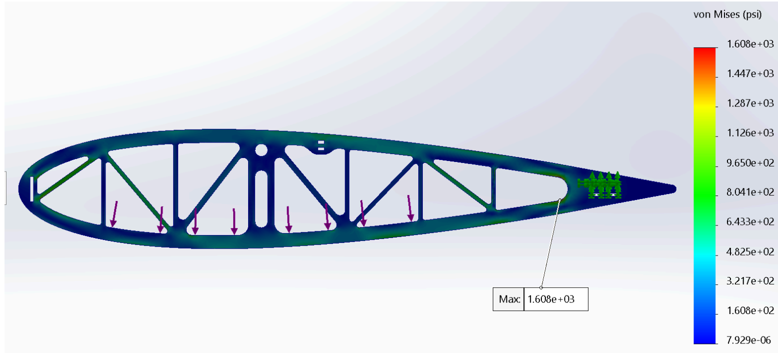

Figure 7.7.1: Bending simulation with load factor of 3 on SolidWorks

The maximum von-Mises stress was determined to be 1.6ksi with an applied load factor of 3 through simulation-driven analysis. This produced a FoS of 2.8, surpassing the conventional 1.2-1.5 to account for plywood's anisotropic nature. To validate this analysis, bending and torsional testing was done on a prototype fuselage. The forward and aft ends were clamped to imitate a beam fixed at both ends. The torsional test showed that the fuselage could resist wing torsion up to a load factor of 3, which UBCAD determined was sufficient to resist torsion. The bending test resulted in excessive buckling and local failure at a load factor of 3.2 and ultimate failure at a load factor of 4.2, giving a FoS of 1.4. UBCAD added more lateral stiffeners to resist buckling and gussets to increase local stiffening and concluded that this was sufficient to resist bending.

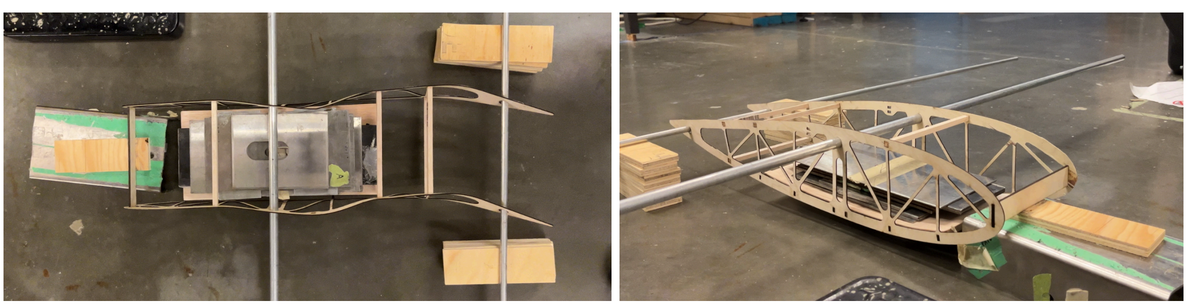

Figure 7.7.2: (left) Excessive buckling behind spar and **(right)** fuselage bending test setup

7.8 Landing Gear Sizing

UBCAD opted for a tricycle LG configuration to optimize short-takeoff capabilities for our thrust-to-weight ratio. To ensure safe landing while maintaining ground maneuverability, the MLG was positioned to withstand 80% of the aircraft's static weight, while the TLG held 20%. This resulted in an overall wheelbase of 16.6", with a track of 13.5". Shock absorption is achieved through the combination of a direct linear spring and elastic wheel deformation. The main legs are swept 25° forward from the vertical to ensure balance and the ability to withstand rough terrain. The MLG springs and wheels can withstand a deflection of 2'' and 0.6'', respectively, providing a total possible vertical stroke of 2.4" at the maximum landing load. Plywood was selected as the primary material for the MLG to minimize weight, and the wing spar was selected as the point of attachment. The 3" wheels are made using 3D-printed thermoplastic and standard PLA. The TLG incorporates a dedicated servo, enabling independent and precise steering control. With a 1.5-inch trail, the TLG ensures stable steering at all speeds, enabling full control in short takeoff and landing scenarios.

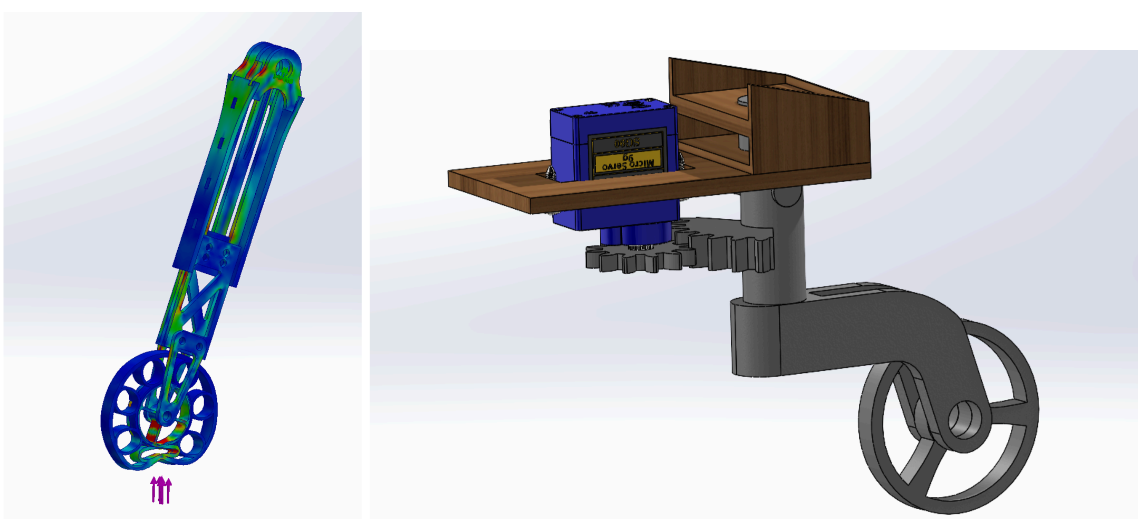

Figure 7.8.1: (Left) Relative stress distribution on the MLG during landing loads & **(right)** Tail landing gear assembly

UBCAD validated prior calculations and ensured safety by conducting static and dynamic testing on the MLG. Using FAR 23.725 standards as a guideline, the MLG was dropped from a simulated height of 7.5” with its static level load corresponding to a controlled free-fall, enabled by the high power-to-weight ratio of the aircraft and its resulting altitude controllability. From multiple tests, the effective spring constant before the full compression of the wheel was determined to be 4.6 lb/in and 13.5 lb/in with and without the wheel respectively.

7.9 Mass properties and balance

Sonic’s layout was designed for the CG and SM to be within ideal target limits for all payload loading configurations [3]. Using preliminary weight estimates from SolidWorks, component positions were iterated until the unloaded configuration of the aircraft met the target limits as outlined in table 7.9.1 . The CG was calculated for various payload loading increments spanning from 0% to 100%. Movement of water during flight causing a shift in CG is a major concern. To prevent such movement, the payload container was selected to be a semi-rigid polyethylene bag modelled as a trapezoidal prism. This bag was customized according to volume calculations and has two ports for filling and draining as shown in figure 7.9.1. This payload design allows for easy switches between payload loading configurations as markings have been made on the bag indicating the fill line for the loading increments. Air is then removed from the remainder of the bag and the empty portion is folded over and sealed to prevent liquid movement. This payload is movable inside the fuselage to accommodate natural CG changes due to loading shifts. The NP and CG can be found in Table 7.9.1 below.

Table 7.9.1: Calculated Neutral Point and Center of Gravity for All Loading Configurations of *Sonic.*

Methods/Parameters	Target	0%	25%	50%	75%	100%
Center of Gravity *(% MAC):*	25% ± 5% [3]	24.93%	24.54%	25.55%	29.76%	24.25%
Neutral Point *(% MAC):*	>28%	36.82% for all loading configurations				
Neutral Point Position *(from datum):*	10.21 ± 0.51 in	10.11 in	10.14 in	10.21 in	9.85 in	10.14 in
Center of Gravity Position *(from datum):*	9.26 ± 0.46 in	9.25 in	9.22 in	9.31 in	9.67 in	9.19 in

The NP was maintained at a distance greater than 2-3% MAC from the CG while computing our SM [3]. From a calculated MTOW of 7.6 lb and an empty weight of 2.6 lb, *Sonic* can carry 5 lb of static payload.

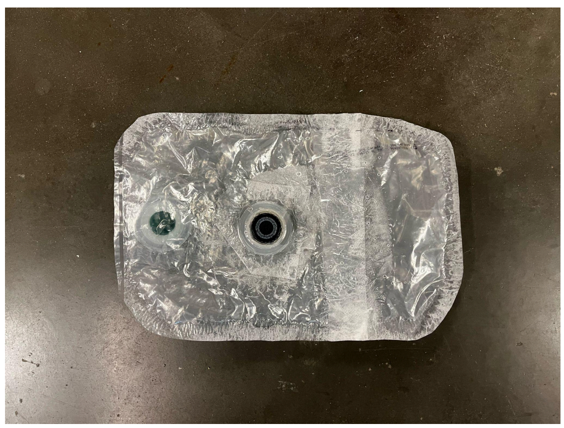

Figure 7.9.1: Payload Container (bag) for *Sonic*

7.10 Static & Dynamic Stability

Static stability was analyzed for varying CG positions, covering all the designed flight envelopes. A VLM analysis on XFLR5 was conducted to obtain C_M versus α values for all lifting surfaces. The results (Figure 7.10.1) indicate that the $C_{M,0}$ is consistently positive for all CG positions analyzed, meeting the stability criteria for C_M at zero lift [1]. Furthermore, for CG positions below 65% x_{CG}/MAC, the C_M slope is consistently negative, fulfilling the static stability criteria [1]. Consequently, Sonic is assured of maintaining static stability throughout all stages of flight.

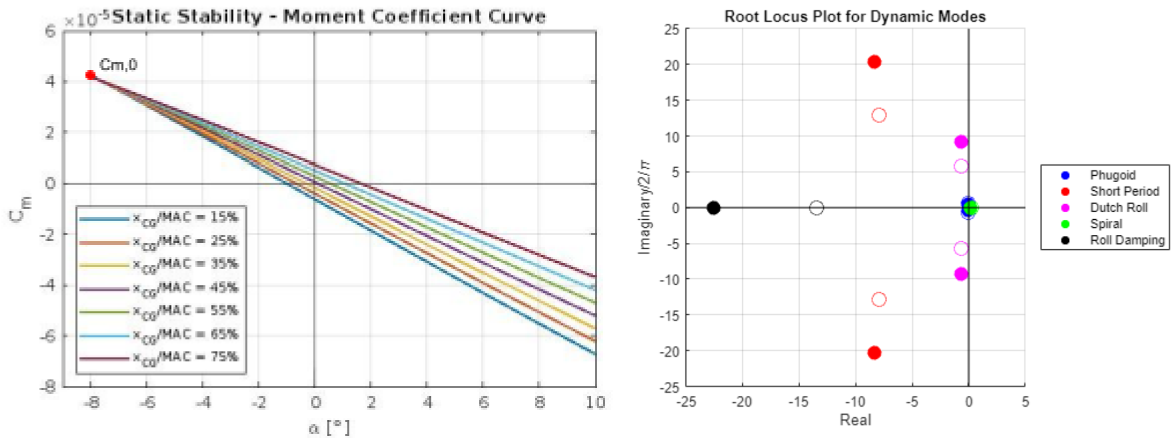

Figure 7.10.1: (left) Static Stability Curve and **(right) Figure 7.10.2** Root Locus Plot of All Dynamic Modes.

UBCAD also analyzed the dynamic stability of our aircraft using XFLR5. A root locus plot was created using XFLR5's eigenmode analysis at critical flight conditions. The analysis neglects the fuselage other than requiring the aircraft's overall inertia and mass properties. The software also translates the eigenvalues into characteristic stability values, which can be compared to the relative "Class 1", "Category B flight phase", and "Level 1 flying qualities" as defined in [11]. Figure 7.10.2 shows the 8 dynamic mode eigenvalues in a root locus plot. The real component negativity implies damping behaviour is present and the imaginary components that oscillatory behaviour is present.

Table 8.3.1 presents the characteristic stability values of our plane against the relative values defined in the military specification document introduced above. All modes other than spiral meet the requirements with acceptable tolerance. The spiral mode fails for t2, the time for the bank angle to double. Therefore the plane is not stable in the spiral mode based on our analysis, but it can be corrected by pilot input through the ailerons.

Table 8.3.1. Characteristic Dynamic Stability Values.

Mode	Characteristic Requirements	*Sonic (Unloaded)*
Phugoid	$\zeta > 0.04$	$\zeta = 0.060$
Short Period	$0.3 < \zeta < 2.0$	$\zeta = 0.522$
Roll	$\tau < 1.4$ sec	$\tau = 0.052$ sec
Dutch Roll	$\zeta > 0.08$ $\omega_N > 0.4$ rad/sec $\zeta*\omega_N > 0.15$ rad/sec	$\zeta = 0.116$ $\omega_N = 5.741$ $\zeta*\omega_N = 0.668$
Spiral	t2 > 20 sec	t2 = 3.374 sec

8. Manufacturing

8.1 Materials

UBCAD selected materials with a high strength-to-density ratio for construction based on the material selection chart [12]. Balsa wood was chosen as the primary construction material for *Sonic* due to its manufacturability, density, cost, and specific strength. Plywood was used for primary structural members such as the large fuselage ribs and wing section interface ribs due to its higher overall strength. Basswood was used for the I-Beam flanges in the HT and VT, due to its cost and high strength-to-density ratio. A CF rod was chosen for the main wing spar, due to its high strength-to-density ratio. The landing gear consists mainly of plywood due to its strength, and PLA/TPU wheels due to TPU's impact absorption properties.

8.2 Methods, techniques and Tools

Sonic has been designed using principles of design for manufacturing and assembly and is built with balsa and plywood that has been precision cut with a laser cutter with tolerances of about five-thousandths of an inch. To ensure the sheeting of the plane conforms exactly to the airfoil shape, this year we used 3D-printed male and female moulds to press the soaked balsa into the exact shape we need, preventing warping and deviation from the airfoil shape. Finally, the outer surfaces of the plane are wrapped in Monokote to reduce the skin friction drag of *Sonic.* During construction, each part is weighed and compared against the CAD to gauge the effectiveness of the construction and validate the CG position.

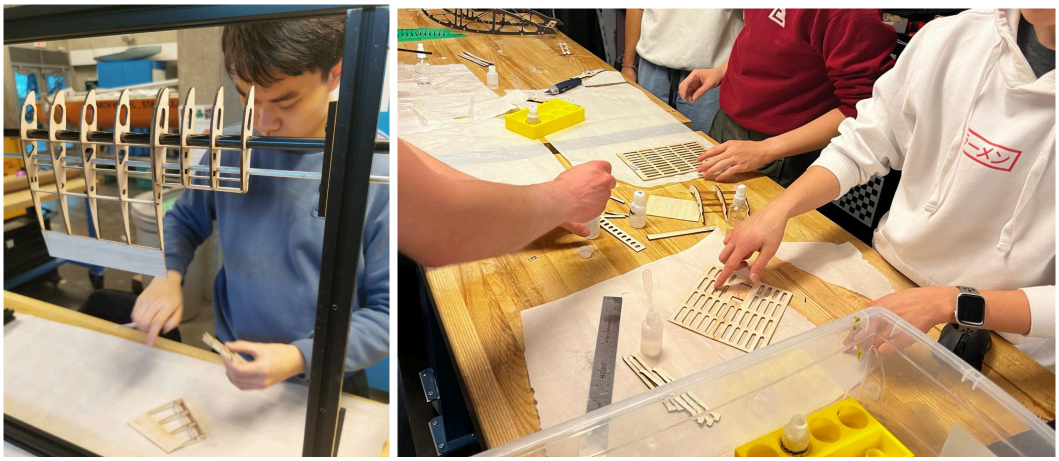

Figure 8.2.1: (left) Manufacturing Wing using Jigs& **(right)** Manufacturing Fuselage with Laser Cut Balsa

9. Conclusion

This year, UBCAD implemented a Model-Based Systems Engineering approach to enhance the scoring algorithm throughout the design process. A well-balanced configuration of wingspan, empty weight, and payload was achieved, resulting in an optimal design. *Sonic*, featuring a 33" wingspan, is tailored for a 7.6lb Maximum Takeoff Weight (MTOW) and is capable of carrying a 5lb static payload, aiming for an expected flight score of 26.12 per flight round. Despite encountering challenges due to a design class change, UBCAD conducted a higher number of iterative physical tests to validate analysis results compared to previous years. Through meticulous analysis, design adjustments, and extensive testing, UBCAD is confident that *Sonic* will emerge as a high-performing aircraft in the upcoming SAE Aero Design West competition.

Due to the nature of a liquid payload in a half-empty container, movement during flight is expected but can be mitigated with astute design choices. The payload container in *Sonic* has a trapezoidal prism shape to minimize shifts in CG and NP during flight. This design choice did prove to be effective as the calculated changes in both the CG and NP are minimal, however can still be minimized further. The effects of a changing angle of attack ranging from -10° to +15° on the neutral point and center of gravity position from the datum (foremost surface of the fuselage) are shown in Figure 1 below. To prevent shifts in these values, the containment method for the payload needed to be flexible so that air could be removed, as this was determined to be the primary cause of water movement, yet rigid enough to maintain its structural integrity. For different loading configurations between 0% and 100% full, the empty portion of the bag is folded over onto itself and temporarily sealed for flight to prevent liquid movement, mimicking a fully loaded bag.

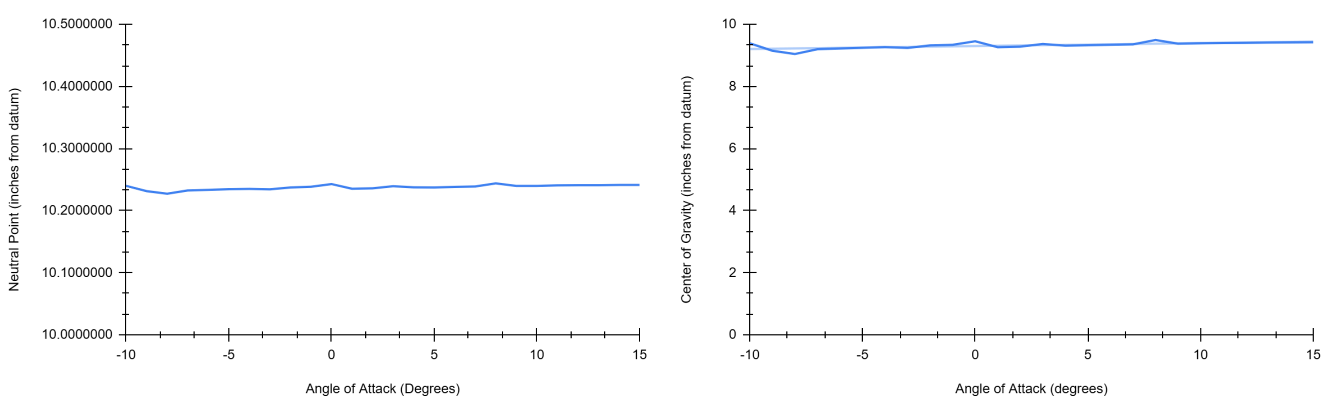

Figure 1: (left) Neutral point position from the datum and **(right)** center of gravity position from the datum with respect to angle of attack with the water payload container half-full